



Contents lists available at ScienceDirect

# Sensors and Actuators A: Physical

journal homepage: [www.elsevier.com/locate/sna](http://www.elsevier.com/locate/sna)



## Electret-material enhanced triboelectric energy harvesting from air flow for self-powered wireless temperature sensor network

Yingchun Wu <sup>a,b</sup>, Yushen Hu <sup>a</sup>, Ziyu Huang <sup>a</sup>, Chengkuo Lee <sup>c</sup>, Fei Wang <sup>a,b,d,\*</sup>

<sup>a</sup> Department of Electrical and Electronic Engineering, Southern University of Science and Technology, Shenzhen, 518055, China

<sup>b</sup> Shenzhen Key Laboratory of 3rd Generation Semiconductor Devices, Shenzhen, 518055, China

<sup>c</sup> Center for Intelligent Sensors and MEMS, National University of Singapore, Singapore

<sup>d</sup> State Key Lab of Transducer Technology, Shanghai Institute of Microsystem and Information Technology, Chinese Academy of Sciences, Shanghai, 200050, China

### ARTICLE INFO

#### Article history:

Received 25 September 2017

Received in revised form

30 December 2017

Accepted 30 December 2017

Available online xxxx

#### Keywords:

Electret materials

Electrostatic energy harvester

Triboelectric generator

Spray coating

Wireless sensor networks

### ABSTRACT

Energy from wind flow is very common in ambient environment which can be harvested by triboelectric generator effectively. Herein, electret based triboelectric generator (E-TriG) with both electrostatic and triboelectric effects are investigated with enhanced performance comparing with the traditional triboelectric generator based on only contact electrification. Electret materials like PTFE, CYTOP, TOPAS, and COC are prepared with different methods and charged under positive or negative conditions to optimize the material property. It is proved that the performance of the triboelectric generator can be improved by negatively charged electrets, while with positively charged electrets, the power output is weakened. As a demonstration, the E-TriG has been successfully applied for wireless temperature sensing. At a wind flow rate of 18 m/s, a storage capacitor can be fully charged by three E-TriGs devices within 15 s, and afterwards, wireless temperature signal could be read and delivered to the internet every 5 s. An average power of 400  $\mu$ W is therefore harvested. With enhanced performance from the corona charged electret, the triboelectric generator shows promising application for the future wireless sensor networks.

© 2018 Elsevier B.V. All rights reserved.

## 1. Introduction

Since the concept of Internet of Things was first proposed by MIT Auto-ID Center in 1999, series of development in this area bring increasing demand for large scale wireless sensor network with high performance. Conventional wireless sensor network cannot work without an external power source like a battery. However, considering the limited lifetime, difficulty for replacement and the severe pollution problem, battery would be the main bottleneck for up-scaling of the wireless sensor networks. Therefore, energy harvester, which can provide sustainable power source, is an ideal solution for large scale application of “intelligent life” with wireless sensor networks. In recent years, the concept of wireless sensor node self-powered by energy harvesting from ambient environment, has been proposed and developed with various functions. Temperature sensing has been extensively applied in many industries and become an indispensable measure of our intelligent life.

For planting, food storage, medicine storage, and central air conditioning system, temperature is a critical factor which needs real-time monitoring. Taking the central air conditioning system as an example, it is promising to scavenge energy from the vibration and air flow in different mechanism, like piezoelectric [1–8], electromagnetic [9–12], electrostatic [13–19] and triboelectric [20–32] generators. For piezoelectric and electrostatic generator, the output is often too limited to support the wireless sensor network; while for electromagnetic generator, the complicated structure and bulky volume limit its application in many scenarios. Since 2012, triboelectric generators (TriG) with different structures have been fabricated for harvesting various types of energy [33–37]. With this mechanism, it is generally believed that the contact/separation between two triboelectric materials drive the electrons flow through the external circuit due to the difference of work function between the two contacting materials.

Although triboelectric generators have been proved to power tens of LEDs [38,39], to charge Li-ion battery [40] and capacitors [24,25] and to power some portable electronics [22,26], researchers are trying to find new way to improve the output for more practical applications: the mass-fabrication technologies like soft lithography process and flexible printed circuit board (i.e., FPCB)

\* Corresponding author at: Department of Electrical and Electronic Engineering, Southern University of Science and Technology, Shenzhen, 518055, China.

E-mail address: [wangf@sustc.edu.cn](mailto:wangf@sustc.edu.cn) (F. Wang).

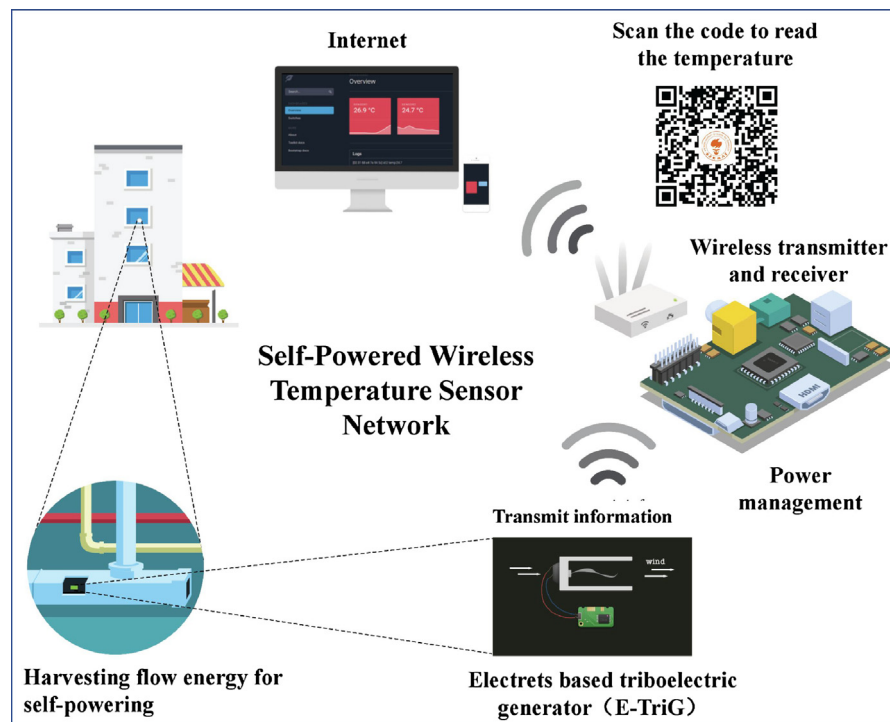


**Fig. 1.** Schematic map of the self-powered wireless temperature sensing system to monitor the temperature of the central air conditioning system, with the energy scavenging from the air flow.

process were used to fabricate flexible and optimized-performed TriG for smart microsystem [27]; ferroelectric polymers was successfully introduced when fabricating the skin-based generator which can easily harvest energy from body motion [28–30]; and graphene/PTFE based generator has been developed to harvest energy from droplet movement [31]. Flapping wing structures with thin film or foil have been designed to scavenge wind flow energy effectively by triboelectric generators [32,40]. And ion injection method [41] which is similar to corona charging method has been used to improve the power output of TriG. Based on the similar structure, we have studied the effect of the electret materials by corona charging [42–44] on the enhanced performance of triboelectric generator, comparing with the normal TriG without the electret materials. Various electret materials like PTFE (polytetrafluoroethylene) film, CYTOP (an amorphous fluoropolymer type: CTL-809M, was purchased from AGC Asahi Glass), TOPAS (thermoplastic polymer mr-IT85), COC (Cyclic olefin copolymer), and PDMS (polydimethylsiloxane) are prepared with different methods and charged under different conditions to explore the optimal choice. It has been proved that the performance of the triboelectric generator can be improved by negatively charged electrets, while with positively charged electrets, the performance is weakened. Furthermore, we have designed an innovative power management circuit for powering temperature wireless sensor network. A schematic illustration has been made to demonstrate the self-powered wireless temperature sensor network which is powered by electrets based TriG (E-TriG) with enhanced performance, as illustrated in Fig. 1. As a demonstration, three E-TriG devices have been connected in parallel to charge a capacitor of 470  $\mu$ F, whose energy can be triggered to release for powering two temperature sensors with power management chip, microcontroller unit (MCU) and transmitter. At a wind flow rate of 18 m/s, the capacitor can be fully charged by the E-TriG devices within 15 s; and afterwards, wireless temperature signals could be delivered to internet every 5 s, which means an average power of 400  $\mu$ W has been harvested.

## 2. Fabrication

### 2.1. Preparation of the electret materials

For PTFE, we used common commercial film as purchased with a thickness of 20  $\mu$ m. For CYTOP, CTL-809 M was purchased from AGC Asahi Glass. We prepared the film by spin coating for 6 cycles, resulting in a final thickness of about 10  $\mu$ m.

For spray coated COC, we prepared the film by a spray coating method. We first mixed the COC/Toluene (5 g/500 ml) solution. Subsequently, the mixed solution was sprayed out from a pipe to a glass substrate by a SC-6 spray coater in the hydraulic power of 0.2 MPa and a sweep power of 0.08 MPa. The substrate was soft baked at 60 °C during the spray coating process. The electret material was then hard-baked at 120 °C for 10 min. The process was repeated for 10 times to get a final thickness of about 60  $\mu$ m.

For spin coated COC, we prepared the film by standard spinning coating method. After full mixture of COC/Toluene (50 g/500 ml), the solution was spin-coated on the glass plate at a speed of 400 rpm for 30 s, and baked at 120 °C for 10 min. We have repeated the process for 10 cycles to obtain 60  $\mu$ m-thick film.

For PDMS, we mixed the PDMS elastomer and cross-linker by 10:1 ratio (W/W). After degassed for 30 min, the mixture was spin-coated on the glass substrate at 500 rpm for 30 s, and finally dried at 90 °C for 90 min.

For TOPAS, we used mr-IT85-20xp Thermoplastic Polymer solution, which was spin-coated at 1000 rpm for 30 s and finally baked at 140 °C for 30 min.

### 2.2. Preparation of the electrodes on electret films and on Kapton film

Cr, Al (50 nm/150 nm) were sputtered successively on both sides of Kapton film (50  $\mu$ m thick) with power of 300 W. Al (150 nm) film was deposited on electret films using the same sputtering process.

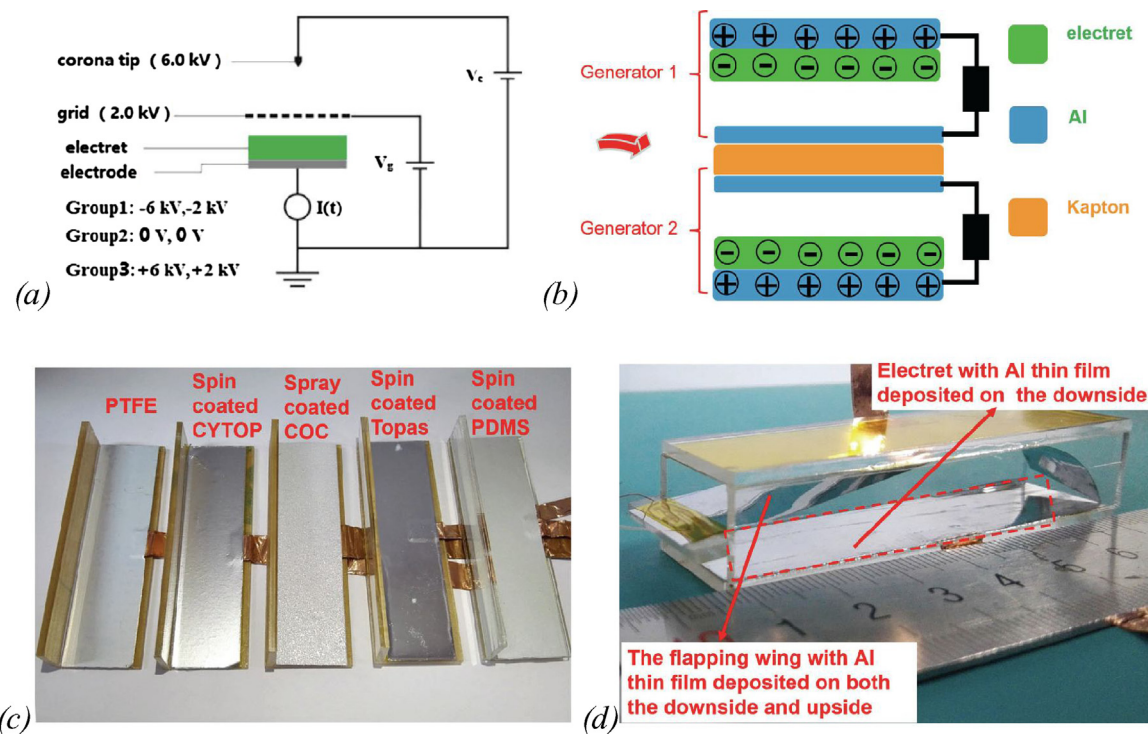


**Fig. 2.** (a)The corona charging setup for electret materials; (b) The structure of E-TriG with two Al-electret pairs for generator 1 (top) and generator 2 (bottom); (c) Image of the electret films and their application in E-TriG: from left to right: PTFE film, spin coated CYTOP film, spray coated COC film, spin coated Topas film and PDMS film; (d) An E-TriG device is assembled with a flapping wing and two counter electret films. The overall size of the E-TriG is 67 mm × 22 mm × 10 mm.

### 2.3. Electret films treatment by corona charging

We used a custom-built corona charging setup as shown in Fig. 2(a): the needle and grid voltages were set to -6 kV (or +6 kV for positive corona charging) and -2 kV (or +2 kV for positive corona charging), respectively. For all the samples, the charging time was 10 min. In this process, charges were deposited into the electret films.

After charging, the surface potential of the electret film was measured by an electrostatic probe. Without charging, the native surface voltage is generally below 100 V, while after charging it can be increased to more than 1000 V for PTFE, CYTOP, and COC. For PDMS, however, we found it can be hardly charged by positive method; therefore, the following test for PDMS is blank for positive corona condition. The samples were stabilized for 3 h before test since the surface charge would naturally decay especially in the first 3 h through our observation. For good comparison, we have prepared three groups of devices for each electret material, with one group charged under negative condition, one under positive condition and one without any charge.

### 2.4. Fabrication of E-TriGs

The E-TriG consists of an electret film and two Al electrodes as sketched in Fig. 2(b). On both sides of a Kapton film (FEP), Al thin films were deposited as electrodes also as one of the contact layers of the triboelectric generator, which will interact with the electret film that has been treated by corona charging. All the components were assembled in an acrylic tube-box of 67 mm × 22 mm × 10 mm with inlet and outlet for air flow. A small acrylic sheet as the bluff body with dimensions of 22 mm × 5 mm × 2 mm was set up at the end of the acrylic tube, on which a Kapton film with the Al electrodes on the two sides was used as the fixed flapping wing. With this structure, two generators (generator 1 and generator 2) can be assembled in one E-TriG device simultaneously. Therefore, the movement of the Kapton film can be utilized more efficiently.

Fig. 2(c) shows the different electret films before assembly and a final E-TriG device for test is shown in Fig. 2(d).

### 3. Work mechanism

The operating principle of the E-TriG can be explained by the coupling effect between contact electrification and electrostatic induction as demonstrated in Fig. 3. To trigger the E-TriGs, an air blower was used to apply wind flow between Al film and electret film which was corona charged with negative surface potential. When driven by external wind, the flapping wing will contact and separate with the electret film, the coupling between triboelectrification and electrostatic induction results in alternating flow of electrons between the electrodes. In the initial state, the Al film (on the flapping wing) is separated from the electret film with a certain distance. As shown in Fig. 3b, the Al film on the flapping wing moves to get approaching towards the electret film according to the wind flow. Because of the electrostatic field from the negative surface charge of the electrets [45], positive charges accumulate on the Al film of the flapping wing through an external circuit (Fig. 3b), which generates the electrostatic induced current. When the Al film comes in contact with the electret film, as shown in Fig. 3c, triboelectric effect dominates between the Al electrode and the electrets polymers. It has been generally believed that due to the work function difference between Al and the polymers [46,47], electrons are injected from top Al electrode to the polymer surface, which generates the triboelectric induced current. When the flapping wing separates from the electret, the amount of the induced charges on the Al electrode decreases which generates a reverse current (Fig. 3d) until the E-TriG flapping wing vibrates to the initial state.

A theoretical analysis was proposed for vibration based electrostatic energy harvester [45,48], which could also be used to calculate the electrostatic induced surface charge:

$$R \frac{dQ_1}{dt} = V - Q_1 \left[ \frac{1}{C_1(t)} + \frac{1}{C_2} \right] \quad (1)$$

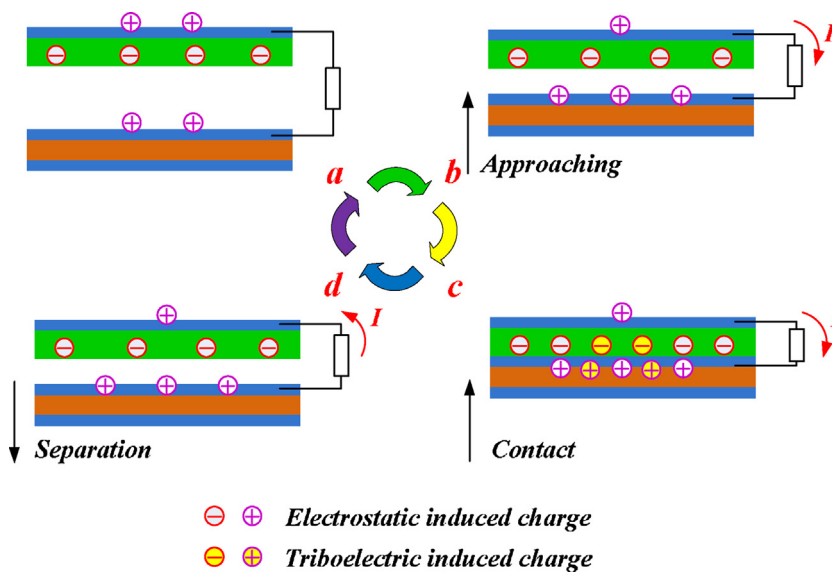


**Fig. 3.** The function mechanism of the electret enhanced triboelectric generator.

where  $Q_1$  is the charge induced on the Al electrode due to electrostatic effect;  $R$  represents the external load resistance;  $V$  stands for the surface potential of the pre-charged electret;  $C_1(t)$  is the capacitance of the air gap and  $C_2$  is the capacitance of the electret material. If we define  $Q_2$  as the charge induced on the Al electrode due to triboelectric effect, the overall charges  $Q_{tot}$  on the Al electrode can be given as:

$$Q_{tot} = Q_1 + Q_2 \quad (2)$$

Based on the mechanism above, it should be noted that the electrostatic induced charge/current and the triboelectric induced charge/current can be added up, only if the electrets are negatively charged ( $Q_1$  and  $Q_2$  have the same sign). When positive charge is applied to the electrets, electrons would be induced instead of positive charges as the flapping wing approaches the electrets film due to the electrostatic field. This electrostatic effect would counteract the triboelectric induced charges during the following contact between the Al film and the electret ( $Q_1$  and  $Q_2$  have the opposite signs).

During our experiment, the flapping movement of the wing was recorded by a high-speed camera, as shown in Fig. S1 and the video in supplementary material. Driven by wind flow of 8 m/s, the wing started approaching the electrets, and charges were induced mainly due to the electrostatic surface potential of the electrets. Once contacting with and separating from the electret surface, the triboelectric effect will work and therefore more charges could be generated.

#### 4. Results and discussion

As shown in Fig. 4a, the device was mounted with an air blower to generate a continuous wind flow with a speed up to 18 m/s during the test, and a commercial anemometer was used to monitor the flow speed during the measurement. Fig. 4b shows the open circuit voltage output of one E-TriG. From the V-t curve, the voltage peak is nearly 60 V when driven by the air flow. It should be noted that the voltage signal of the lower device is mirrored top-down for better comparison.

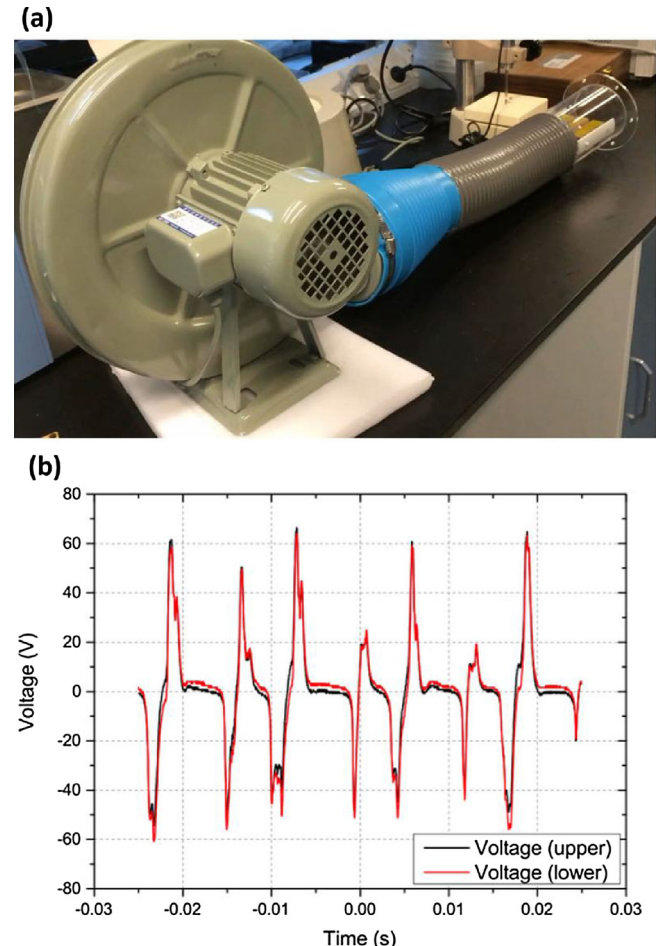


**Fig. 4.** (a) An air blower is used to generate the wind flow, and a commercial anemometer is used to monitor the flow rate during the measurement. (b) Open circuit voltage output of one E-TriG prior to rectifying. Each E-TriG device is composed of an upper device (generator 1) and a lower device (generator 2), which can improve the overall power output. It should be noted that the voltage signal of the lower device is mirrored top-down for better comparison.

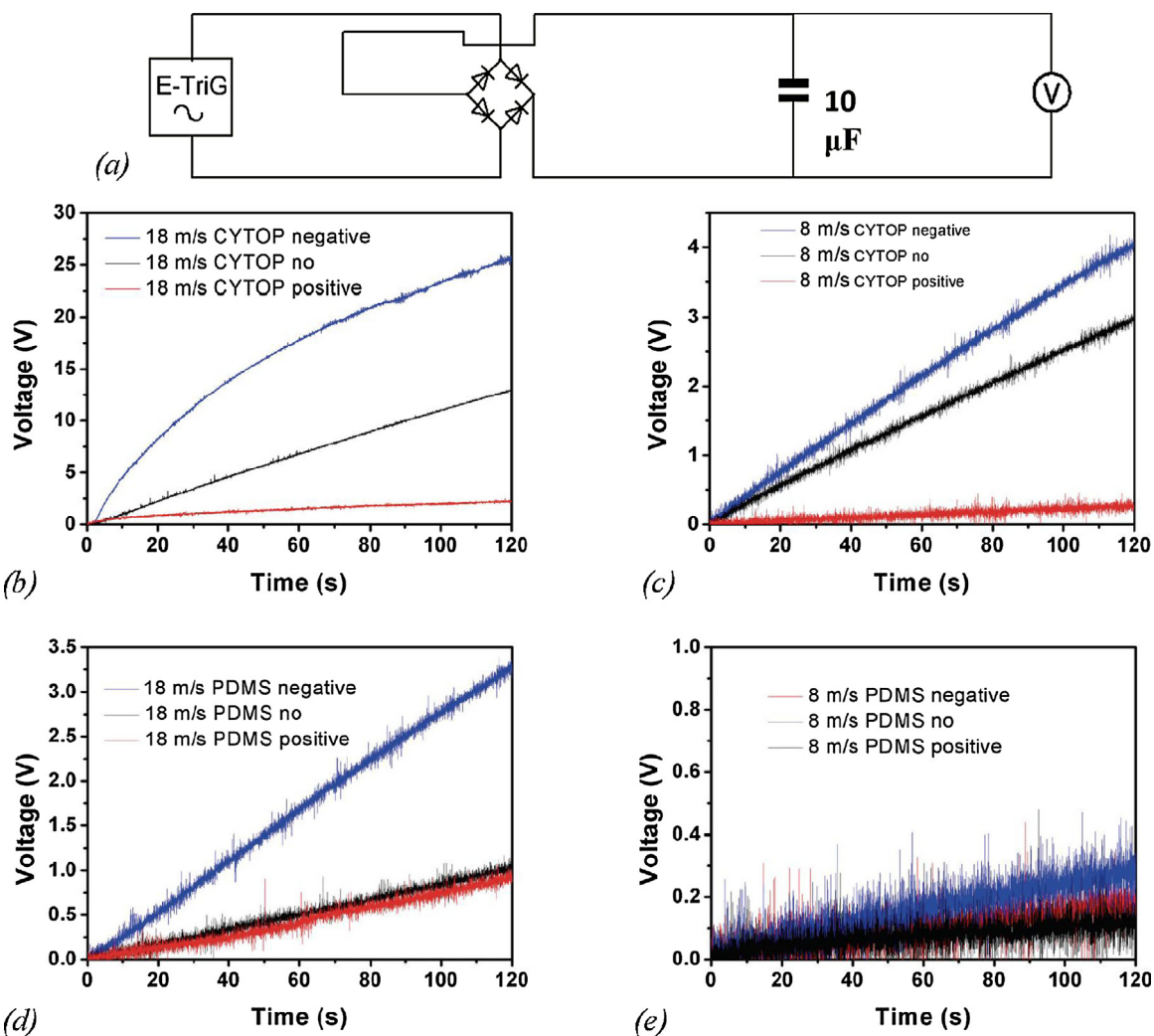


**Fig. 5.** (a) Test circuit for the E-TriG with a rectifier and charging capacitor; Capacitor charging performance from E-TriG devices with electret materials of (b–c) CYTOP; (d,e) PDMS under two wind speeds of 18 m/s and 8 m/s, respectively.

#### 4.1. Comparison of different corona charging condition

As shown in Fig. 5a, the E-TriG devices were characterized by testing the charging performance for a capacitor of 10  $\mu$ F. We can calculate the power output of the device by measuring the voltage across the capacitor. The voltage of the capacitor was measured by a Keithley electrometer (Keithley 6514). The maximum voltage and the charging speed can be measured to evaluate the enhancement by the electrets. The three corona charging conditions for the electret films can also be compared.

It is observed that all of the generators can charge the capacitor successfully under flow rates of 18 m/s and 8 m/s. Plots in Fig. 5(b–e) show the performance of E-TriG devices with CYTOP and PDMS on charging the capacitor. With wind flow of 18 m/s, for the E-TriG with negative charged CYTOP, the voltage of the capacitor can reach 25.6 V in about 2 min, while for CYTOP without being charged, the capacitor can be charged to only 12.97 V. It means that when CYTOP electret film is charged by negative condition, the E-TriG can harvest energy more efficiently; therefore, the capacitor can be charged faster comparing with the E-TriG without being charged. On the contrary, the E-TriG with positive charge exhibits the worst performance, which gets only 2.26 V during the same period. The E-TriGs based on PDMS film get similar results as those with CYTOP film when tested in different wind speeds.

The charging stability of the electrets were investigated by measuring the voltage of the same capacitor charged by the E-TriG devices during the period of 120 s, as shown in Fig. 6(a) and (b). The comparison can be more clearly seen from the histograms shown in Fig. 6(c) and (d) for wind speed of 8 m/s and 18 m/s, respectively. The results indicate that, for all the E-TriG devices, the capacitor can always be charged fastest when the electret film is negatively charged. And for the E-TriG with positive charged film, the charging performance is worst. As discussed above, this might due to the fact that Al tends to get positive charge during the contact electrification, which could be counteracted by the positive surface charge of the electrets. It should be noted that the enhancement of the TENG is dependent on the electrets materials. Taking the spray coated COC polymer as an example, the output voltage of the device is enhanced by ~6 times at a wind speed of 18 m/s, as shown in Fig. 6(d). For PTFE and CYTOP electrets, this enhancement is not so significant because the output voltage of the pure TENG is already very high. More comparison on the energy storage capacity and charging speed for the capacitor has been investigated under more flow rates of 9.2 m/s, 11.2 m/s, 14 m/s, in addition to 8 m/s and 18 m/s. Among all the electrets under study, PTFE and CYTOP demonstrate better performance; while PDMS and TOPAS are seemed to be unsuitable for E-TriG application. Therefore negative corona charging for PTFE or CYTOP can provide a highly

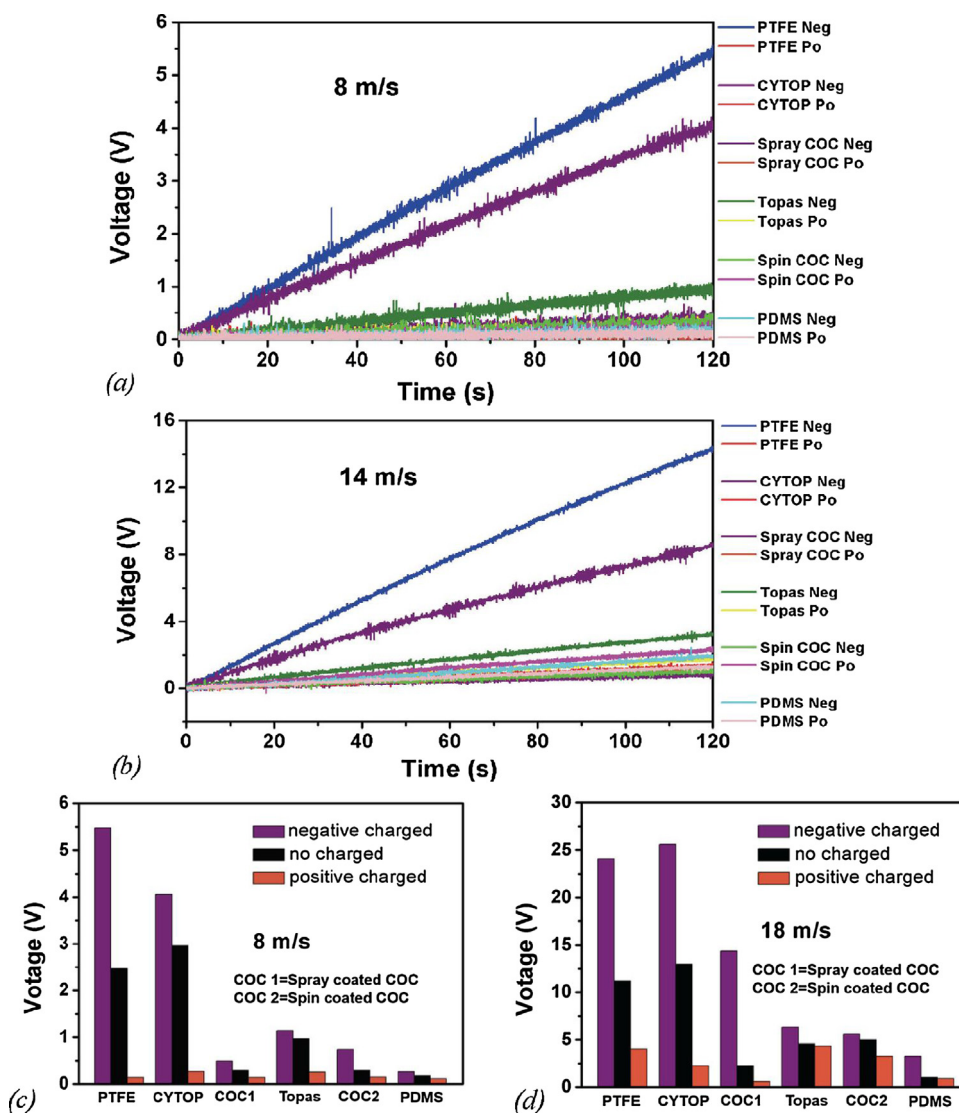


**Fig. 6.** Capacitor charging performance from E-TriG devices under different wind speeds of (a) 8 m/s; (b) 14 m/s with electret materials of PTFE; CYTOP; Spray-coated COC (COC1); Spin-coated TOPAS; Spin-coated COC (COC2) and PDMS; (c,d) Statistic comparison among the electrets with different charging conditions with wind speeds of 8 m/s and 18 m/s, respectively.

effective way to enhance the output performance of triboelectric generator.

#### 4.2. Application for self-powered temperature sensor network

A self-powered temperature sensor network was illustrated in Fig. 7(a), showing the basic system architecture from the wireless sensor node to the gateway. The detailed circuits are shown in Fig. S3. Powered by our E-TriGs, the power management waits for charging of the storage caps (Cs) at the beginning. When the voltage of Cs reaches the set threshold, a trigger signal is sent and the storage energy is partly released to provide the power supply for a microcontroller unit (MCU). Then the MCU reads the surrounding temperature, and encodes the signal. The encoded data is conveyed to a transmitter, which can send out the wireless signal with the temperature information. On the other side, a wireless receiver decodes the information and transfers the signal to a Raspberry Pi, which delivers the message to the gateway. Finally, the temperature message will be displayed on the website and people can monitor the temperature in real-time with a laptop or a smart

phone. The function algorithm of the self-powered wireless sensing system is shown in Fig. S4.

A prototype of the self-powered wireless sensor node is shown in Fig. 7(b)–(e). Together with three E-TriGs of PTFE electret, all the components of rectifiers, MCU, power management chip, temperature sensors and transmitter were installed in a plastic pipe to mimic the tunnel of a central air-conditioning system. The charge and discharge profiles of the Co and Cs in the power management chip were recorded by a digital oscilloscope (DSO9104A). A temperature sensor (Si7055) and a power management chip LTC3588-1 were utilized in the demonstration of the wireless sensor node.

Fig. 8 shows the voltage on the storage capacitor (Cs) and the output capacitor (Co). It took about 15 s to charge the Cs to a threshold voltage of 4.2 V, and then released part of the energy in Cs to charge the output capacitor (Co) to 1.8 V quickly. After the first cycle of charging (cold start), it only took about 5 s for the following wireless sensing and signal transmitting process. Based on the voltage change of Cs, an average power output of 400  $\mu$ W is calculated for the three E-TriGs. In Fig. S5, we demonstrated the application for two wireless temperature sensors network powered by the E-TriGs,

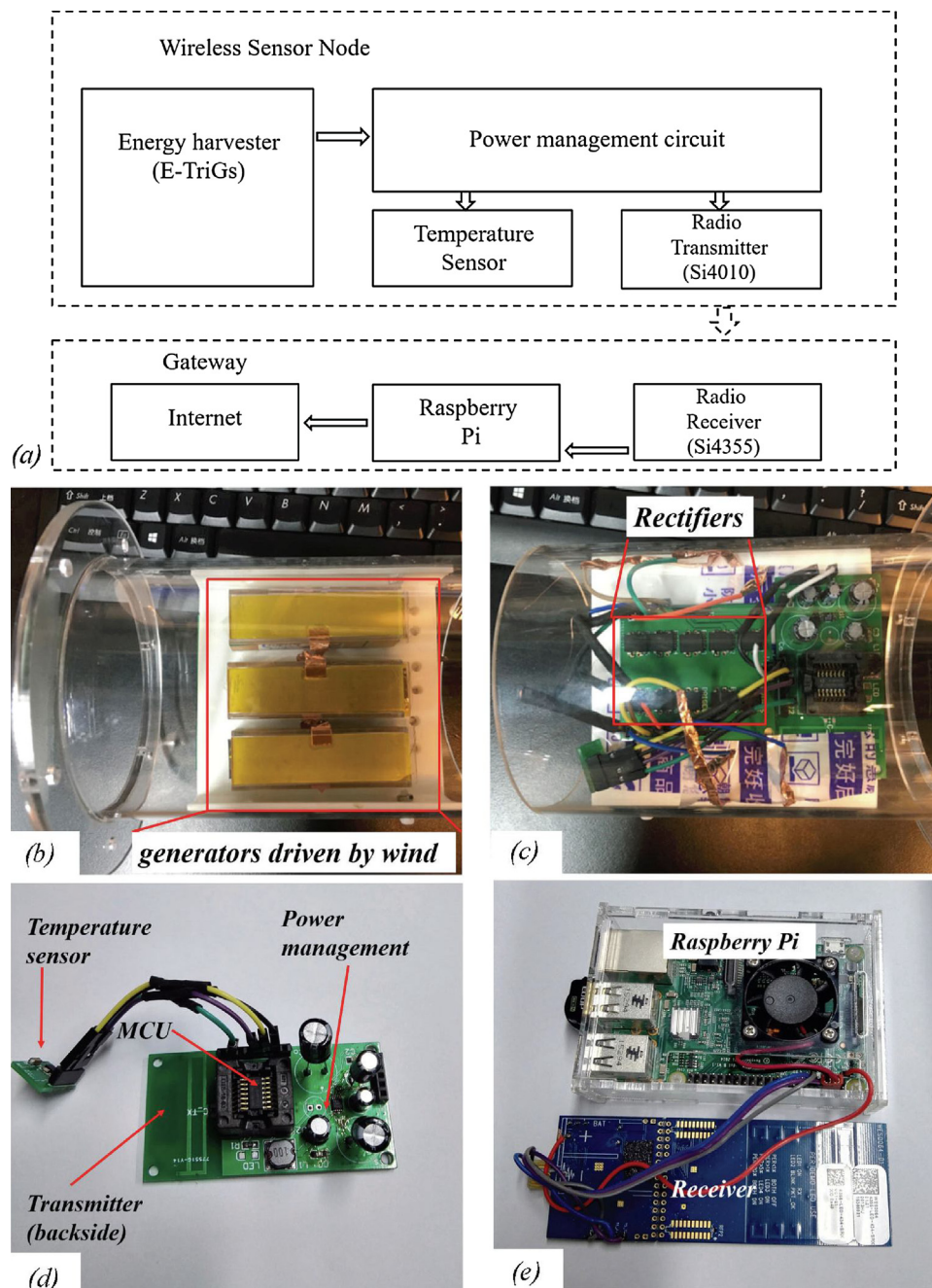


**Fig. 7.** (a) The diagram of a wireless temperature sensing system with self-powered wireless sensor node and gateway. (b) Three E-TriGs are mounted to generate electric power from air flow for the wireless sensor node; (c) The AC voltage output of the E-TriGs are tuned by a series of rectifiers; (d) The main PCB board consists of a microcontroller unit (MCU, Si4010), power management chip (LTC3588-1), temperature sensor (Si7055) and transmitter on the backside of the board; (e) Si4355 is used to receive the wireless temperature signal which is delivered to the internet by a Raspberry Pi.

and the temperature information in our lab can easily be accessed with a smartphone via the barcode.

## 5. Conclusion

In this paper, triboelectric generators base on charged electret film with enhanced power output have been developed to scavenge energy from the air flow to power wireless temperature sensor nodes. The mechanism of E-TriG has been studied and verified by experiments. Different types for electret materials such as PTFE, CYTOP, spray coated COC, spin coated COC, Topas and PDMS have been prepared to fabricate the thin films for the ETriG application. We have proved that for all the electret materials, the

E-TriG performance can be improved by negative charging, while with positive charging, the device performance could be weakened. Furthermore, we have applied the E-TriG device with PTFE electret for an integrated wireless sensing system which consists of power management chip, MCU, storage capacitors, temperature sensors, transmitter, receiver, and gateway. Powered by three E-TriG devices, this system can acquire temperature signal and deliver the information to the internet every 5 s, after a cold start process of 15 s. The enhanced performance of the triboelectric generators by electret materials demonstrates promising application for battery-free wireless sensor networks in the future.

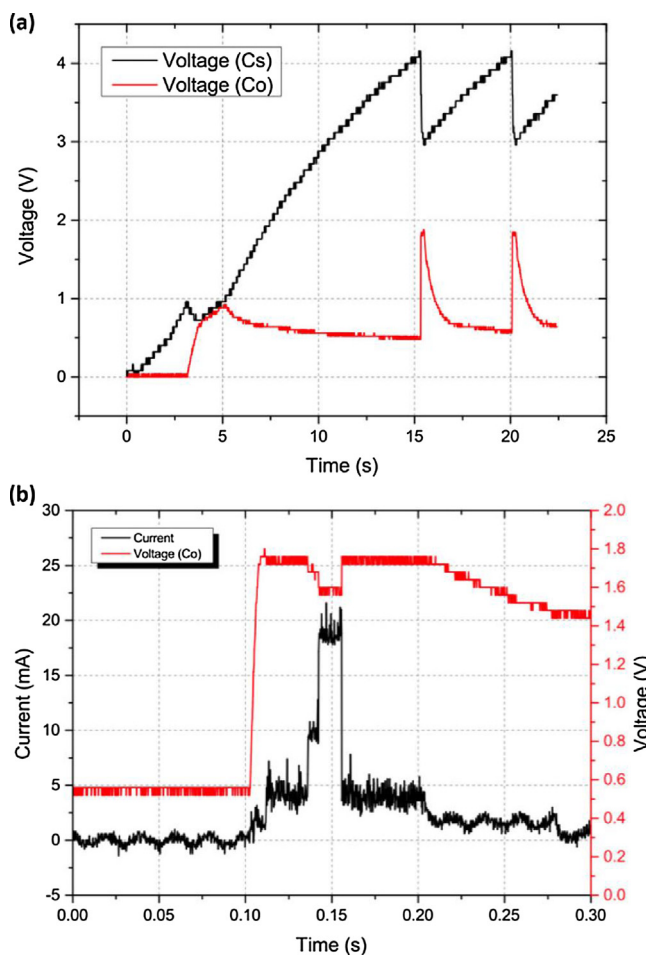


**Fig. 8.** (a) V-t curves for Cs for energy storage and Co for providing a trigger signal to set the mode of the power management; (b) Closed-up view of the voltage and current of Co, showing the generation of the trigger signal.

## Acknowledgements

This work was supported by National Natural Science Foundation of China (Project No.: 51505209) and Shenzhen Science and Technology Innovation Committee (Projects Nos.: JCYJ20170412154426330 and KQTD2015071710313656). Fei Wang is also supported by Guangdong Natural Science Funds (Project Nos.: 2015A030313812 and 2016A030306042) and the Guangdong Special Support Program (Project No.: 2015TQ01X555).

## Appendix A. Supplementary data

Supplementary material related to this article can be found, in the online version, at doi: <https://doi.org/10.1016/j.sna.2017.12.067>.

## References

- [1] L. Gu, C. Livermore, Passive self-tuning energy harvester for extracting energy from rotational motion, *Appl. Phys. Lett.* 97 (August (8)) (2010) 081904.
- [2] S. Li, Z. Peng, A. Zhang, F. Wang, Dual resonant structure for energy harvesting from random vibration sources at low frequency, *AIP Adv.* 6 (January) (2016) 015019.
- [3] E.E. Aktakka, R.L. Peterson, K. Najafi, A CMOS-compatible piezoelectric vibration energy scavenger based on the integration of bulk PZT films on silicon, in: 2010 IEEE International Electron Devices Meeting (IEDM), December, 2010.
- [4] R. Elfrink, T.M. Kamel, M. Goedbloed, S. Matova, D. Hohlfeld, R. van Schaijk, R. Vullers, Vibration energy harvesting with aluminum nitride-based piezoelectric devices, *J. Micromech. Microeng.* 19 (August) (2009) 094005.
- [5] D. Shen, J.H. Park, J. Ajitsaria, S.Y. Choe, H.C. Wikle, D.J. Kim, The design, fabrication and evaluation of a MEMS PZT cantilever with an integrated Si proof mass for vibration energy harvesting, *J. Micromech. Microeng.* 18 (April) (2008) 055017.
- [6] Q.C. Tang, Y.L. Yang, X.X. Li, Bi-stable frequency up-conversion piezoelectric energy harvester driven by non-contact magnetic repulsion, *Smart Mater. Struct.* 20 (November) (2011) 125011.
- [7] H. Liu, C.J. Tay, C. Quan, T. Kobayashi, C. Lee, Piezoelectric MEMS energy harvester for low-frequency vibrations with wideband operation range and steadily increased output power, *J. Microelectromech. Syst.* 20 (October) (2011) 1131–1142.
- [8] S. Li, A. Crovetto, Z. Peng, A. Zhang, O. Hansen, M. Wang, X. Li, F. Wang, Bi-resonant structure with piezoelectric PVDF films for energy harvesting from random vibration sources at low frequency, *Sensor Actuat. A: Phys.* 247 (2016) 547–554.
- [9] P. Constantinou, P.H. Mellor, P.D. Wilcox, A magnetically sprung generator for energy harvesting applications, *IEEE/ASME Trans. Mechatron.* 17 (3) June (2012) 415–424.
- [10] A.R.Md. Foisal, C. Hong, G.S. Chunga, Multi-frequency electromagnetic energy harvester using a magnetic spring cantilever, *Sensor Actuat. A: Phys.* 182 (May) (2012) 106–113.
- [11] B. Yang, C. Lee, Non-resonant electromagnetic wideband energy harvesting mechanism for low frequency vibrations, *Microsyst. Technol.* 16 (March) (2010) 961–966.
- [12] E. Sardini, M. Serpelloni, An efficient electromagnetic power harvesting device for low-frequency applications, *Sensor Actuat. A: Phys.* 172 (September) (2011) 475–482.
- [13] H. Lo, Y.C. Tai, Parylene-based electret power generators, *J. Micromech. Microeng.* 18 (2008) 104006.
- [14] S. Boisseau, G. Despesse, T. Ricart, E. Defay, A. Sylvestre, Cantilever-based electrets energy harvesters, *Smart Mater. Struct.* 20 (2011) 105013.
- [15] T. Takahashi, M. Suzuki, T. Nishida, Y. Yoshikawa, S. Aoyagi, Vertical capacitive energy harvester positively using contact between proof mass and electret plate - stiffness matching by spring support of plate and stiction prevention by stopper mechanism, *28th IEEE International Conference on Micro Electro Mechanical Systems (MEMS 2015)* (2015) 1145–1148.
- [16] A. Crovetto, F. Wang, O. Hansen, An electret-based energy harvesting device with a wafer-level fabrication process, *J. Micromech. Microeng.* 23 (October) (2013) 114010.
- [17] F. Wang, O. Hansen, Electrostatic energy harvesting device with out-of-the-plane gap closing scheme, *Sensor Actuat. A: Phys.* 211 (March) (2014) 131–137.
- [18] Y. Chiu, Y.C. Lee, Flat and robust out-of-plane vibrational electret energy harvester, *J. Micromech. Microeng.* 24 (December) (2013) 015012.
- [19] R. Guillemet, P. Basset, D. Galayko, F. Cottone, F. Marty, T. Bourouina, Wideband MEMS electrostatic vibration energy harvesters based on gap-closing interdigitated combs with a trapezoidal cross section, *26th International Conference on Micro Electro Mechanical Systems (MEMS) (2013)* 817–820, March.
- [20] C. Zhang, T. Zhou, W. Tang, C. Han, L. Zhang, Z.L. Wang, Rotating-disk-based direct-current triboelectric nanogenerator, *Adv. Energy Mater.* 4 (2014), 1301798-n/a.
- [21] M. Ma, Q. Liao, G. Zhang, Z. Zhang, Q. Liang, Y. Zhang, Self-recovering triboelectric nanogenerator as active multifunctional sensors, *Adv. Funct. Mater.* 25 (2015) 6489–6494.
- [22] T. Quan, Y. Wu, Y. Yang, Hybrid electromagnetic–triboelectric nanogenerator for harvesting vibration energy, *Nano Res.* 8 (2015) 3272–3280.
- [23] B. Yu, M. Han, H. Chen, Z. Su, J. Zhang, H. Zhang, Jagged discharge electrodes powered by triboelectric generator, *Micro Nano Lett.* 10 (2015) 537–540.
- [24] Y. Wu, X. Wang, Y. Yang, Z.L. Wang, Hybrid energy cell for harvesting mechanical energy from one motion using two approaches, *Nano Energy* 11 (2015) 162–170.
- [25] Y. Wu, X. Zhong, X. Wang, Y. Yang, Z.L. Wang, Hybrid energy cell for simultaneously harvesting wind, solar, and chemical energies, *Nano Res.* 7 (2014) 1631–1639.
- [26] S. Wang, L. Lin, Z.L. Wang, Nanoscale triboelectric-effect-enabled energy conversion for sustainably powering portable electronics, *Nano Lett.* 12 (2012) 6339–6346.
- [27] X.-S. Zhang, M.-D. Han, B. Meng, H.-X. Zhang, High performance triboelectric nanogenerators based on large-scale mass-fabrication technologies, *Nano Energy* 11 (2015) 304–322.
- [28] J.-H. Lee, R. Hinchet, T.Y. Kim, H. Ryu, W. Seung, H.-J. Yoon, et al., Control of skin potential by triboelectrification with ferroelectric polymers, *Adv. Mater.* 27 (2015) 5553–5558.
- [29] Q. Shi, H. Wang, T. Wang, C. Lee, Self-powered liquid triboelectric microfluidic sensor for pressure sensing and finger motion monitoring applications, *Nano Energy* 30 (2016) 450–459.
- [30] L. Dhakar, P. Pitchappa, F.E.H. Tay, C. Lee, An intelligent skin based self-powered finger motion sensor integrated with triboelectric nanogenerator, *Nano Energy* 19 (2016) 532–540.
- [31] S.S. Kwak, S. Lin, J.H. Lee, H. Ryu, T.Y. Kim, H. Zhong, et al., Triboelectrification-induced large electric power generation from a single moving droplet on graphene/polytetrafluoroethylene, *Acs Nano* 10 (2016) 7297–7302.

- [32] S. Wang, X. Mu, Y. Yang, C. Sun, A.Y. Gu, Z.L. Wang, Flow-driven triboelectric generator for directly powering a wireless sensor node, *Adv. Mater.* 27 (2015) 240–248.
- [33] W. Xu, L.-B. Huang, M.-C. Wong, L. Chen, G. Bai, J. Hao, Environmentally Friendly hydrogel-based triboelectric nanogenerators for versatile energy harvesting and self-powered sensors, *Adv. Energy Mater.* 7 (2017), 1601529-n/a.
- [34] G. Cheng, Z.-H. Lin, L. Lin, Z.-I. Du, Z.L. Wang, Pulsed nanogenerator with huge instantaneous output power density, *Acs Nano* 7 (2013) 7383–7391.
- [35] J. Yang, J. Chen, Y. Yang, H. Zhang, W. Yang, P. Bai, et al., Broadband vibrational energy harvesting based on a triboelectric nanogenerator, *Adv. Energy Mater.* 4 (2014), n/a-n/a.
- [36] F.-R. Fan, L. Lin, G. Zhu, W. Wu, R. Zhang, Z.L. Wang, Transparent triboelectric nanogenerators and self-powered pressure sensors based on micropatterned plastic films, *Nano Lett.* 12 (2012) 3109–3114.
- [37] S. Wang, Y. Xie, S. Niu, L. Lin, Z.L. Wang, Freestanding triboelectric-layer-based nanogenerators for harvesting energy from a moving object or human motion in contact and non-contact modes, *Adv. Mater.* 26 (2014) 2818–2824.
- [38] H. Guo, Z. Wen, Y. Zi, M.-H. Yeh, J. Wang, L. Zhu, et al., A water-proof triboelectric-electromagnetic hybrid generator for energy harvesting in harsh environments, *Adv. Energy Mater.* 6 (2016), 1501593-n/a.
- [39] Y. Yang, H. Zhang, R. Liu, X. Wen, T.C. Hou, Z.L. Wang, Fully enclosed triboelectric nanogenerators for applications in water and harsh environments, *Adv. Energy Mater.* 3 (2013) 1563–1568.
- [40] Y. Yang, G. Zhu, H. Zhang, J. Chen, X. Zhong, Z.-H. Lin, et al., Triboelectric nanogenerator for harvesting wind energy and as self-powered wind vector sensor system, *Acs Nano* 7 (2013) 9461–9468.
- [41] S. Wang, Y. Xie, S. Niu, L. Lin, C. Liu, Y.S. Zhou, et al., Maximum surface charge density for triboelectric nanogenerators achieved by ionized-air injection: methodology and theoretical understanding, *Adv. Mater.* 26 (2014) 6720–6728.
- [42] F. Wang, C. Bertelsen, G. Skands, T. Pedersen, O. Hansen, Reactive ion etching of polymer materials for an energy harvesting device, *Microelectron. Eng.* 97 (2012) 227–230.
- [43] Y. Xu, et al., Spray coating of polymer electret with nano particles for electrostatic energy harvesting, *Micro Nano Lett.* 11 (2016) 640–644.
- [44] Y. Zhang, et al., Electrostatic energy harvesting device with dual resonant structure for wideband random vibration sources at low frequency, *Rev. Sci. Instrum.* 87 (2016) 125001.
- [45] A. Crovetto, F. Wang, O. Hansen, Modeling and optimization of an electrostatic energy harvesting device, *IEEE/ASME J. Microelectromech. Syst.* 23 (5) (2014) 1141–1155.
- [46] C.F. Gallo, W.L. Lama, Some charge exchange phenomena explained by a classical model of the work function, *J. Electrostat.* 2 (June (2)) (1976) 145–150.
- [47] Lieng-Huang Lee, Dual mechanism for metal-polymer contact electrification, *J. Electrostat.* 32 (1994) 1–29.
- [48] Y. Zhang, T. Wang, A. Luo, Y. Hu, X. Li, F. Wang, Micro electrostatic energy harvester with both broad bandwidth and high normalized power density, *Appl. Energy* 212 (2018) 362–371.

## Biographies

**Yingchun Wu** received the B.S. degrees Materials in Science and Engineering Xiangtan University, Xiangtan, Hunan, China, in 2012, and the M.S. degree in Materials in Engineering from University of Chinese Academy of Sciences, Beijing, China, in 2015. She is currently an engineer with the Southern University of Science and Technology, Guangdong, China.

**Yushen Hu** is currently pursuing the bachelor's degree with the Department of Electronic and Electrical Engineering, Southern University of Science and Technology, China. His current research interests include circuit design and test for energy harvesters and self-powered wireless sensor network system.

**Ziyu Huang** is currently pursuing the bachelor's degree with the Department of Electronic and Electrical Engineering, Southern University of Science and Technology, China. His current research interests include energy harvesters and self-powered sensors.

**Chengkuo Lee** is the Director of Center for Intelligent Sensors and MEMS at National University of Singapore. He received M.Sc., in Department of Materials Science & Engineer, National Tsing Hua University in 1991, and M.Sc., in Department of Industrial & System Engineering, the State University of New Jersey in 1993, and Ph.D., in Department of Precision Engineering, University of Tokyo in 1996. His research interest covers energy harvesting, nanophotonics and MEMS.

**Fei Wang** received the B.S. degree in mechanical engineering from the University of Science and Technology of China, Hefei, China, in 2003, and the Ph.D. degree in microelectronics from Shanghai Institute of Microsystem and Information Technology, Chinese Academy of Science, Shanghai, China, in 2008. He was a Postdoctoral Researcher with the Department of Microtechnology and Nanotechnology, Technical University of Denmark, where he had been promoted to assistant professor since 2010. Since 2013, he has been an associate professor in the department of Electronic and Electrical Engineering, Southern University of Science and Technology, China. His current research interests include micro energy harvesting, MEMS and NEMS devices, IC and semiconductor testing. Dr. Wang served as a TPC Member for the 19th International Conference on Solid-State Sensors, Actuators and Microsystems (Transducers 2017), the International Conference on Manipulation, Manufacturing and Measurement on the Nanoscale (IEEE 3M-NANO) from 2014 to 2017, and the International Multidisciplinary Conference on Optofluidics (Optofluidics) from 2016 to 2017.